王汇, 穆歆迪, 苏婷婷, 等. 藜麦 RS3 型抗性淀粉的理化性质及其体外发酵对肠道菌群和代谢物的影响 [J]. 食品工业科技, 2026, 47(12): 12−26. doi: 10.13386/j.issn1002-0306.2025090023

WANG Hui, MU Xindi, SU Tingting, et al. Physicochemical Properties of Quinoa RS3 Resistant Starch and Its Effects on Intestinal Flora and Metabolites during *in Vitro* Fermentation[J]. Science and Technology of Food Industry, 2026, 47(12): 12−26. (in Chinese with English abstract). doi: 10.13386/j.issn1002-0306.2025090023

·特邀主编专栏—植物基食品原料基础研究、前沿技术创新及其健康绿色产品开发（客座主编：于寒松、张健、李健）·

藜麦 RS3 型抗性淀粉的理化性质及其体外发酵对肠道菌群和代谢物的影响

王　汇[1], 穆歆迪[1], 苏婷婷[1], 杨惜媛[1], 徐　磊[1], 姚　笛[1,2,3,*], 王长远[1,3,*], 张丽媛[1,2,3]

（1.黑龙江八一农垦大学食品学院, 黑龙江大庆 163319;
2.黑龙江省农产品加工与质量安全重点实验室, 黑龙江大庆 163319;
3.国家杂粮工程技术中心, 黑龙江大庆 163319）

摘　要: 为了解藜麦 RS3 型抗性淀粉（quinoa resistant starch，QRS）的理化性质及体外发酵对肠道菌群和短链脂肪酸（short-chain fatty acids，SCFAs）的影响，本研究以藜麦为原料，采用碱浸提法制备藜麦淀粉（quinoa starch，QS），并通过压热法对其进一步处理得到 RS3 型 QRS。然后对二者的直链淀粉含量、透光率、糊化特性和热特性等理化性质进行研究，并利用体外粪便模拟发酵体系、16S rRNA 测序和液相色谱-质谱联用非靶向代谢组学技术，进一步探究了二者的体外发酵特性及对肠道代谢物的影响。结果表明，与 QS 相比，RS3 型 QRS 的抗性淀粉（QRS）含量和直链淀粉含量显著增加（$P<0.05$）；透光性和溶解性显著提高（$P<0.05$）；具有更稳定的热力学性质，且更容易烹饪，品质更好。在体外发酵基质中添加 RS3 型 QRS 后，普氏栖粪杆菌（*Faecalibacterium*）丰度增加，志贺氏菌（*Escherichia-Shigella*）丰度降低。RS3 型 QRS 的核心群落厚壁菌门（Firmicutes），包括布劳特氏菌（*Blautia*）、乳球菌属（*Lactococcus*），它们与丁酸的富集呈显著正相关（$P<0.01$ 或 $P<0.05$）；与胆汁分泌代谢途径相关的胆汁酸水平显著提高（$P<0.05$）。肠道菌群产生的 SCFAs 与这些差异代谢物共同维持了肠道稳态。本研究将为探究 RS3 型 QRS 对肠道健康的影响提供参考价值，为 RS3 型 QRS 的应用提供理论依据。

关键词: 藜麦, RS3 型抗性淀粉, 体外发酵, 肠道菌群, 代谢物, 胆汁酸

中图分类号: TS201.3　　**文献标识码:** A　　**文章编号:** 1002−0306(2026)12−0012−15

DOI: 10.13386/j.issn1002-0306.2025090023　　本文网刊:

Physicochemical Properties of Quinoa RS3 Resistant Starch and Its Effects on Intestinal Flora and Metabolites during *in Vitro* Fermentation

WANG Hui[1], MU Xindi[1], SU Tingting[1], YANG Xiyuan[1], XU Lei[1], YAO Di[1,2,3,*], WANG Changyuan[1,3,*], ZHANG Liyuan[1,2,3]

（1.College of Food, Heilongjiang Bayi Agricultural University, Daqing 163319, China;
2.Key Laboratory of Agroproducts Processing and Quality Safety of Heilongjiang Province, Daqing 163319, China;
3.National Coarse Cereals Engineering Research Center, Daqing 163319, China）

Abstract: To understand the physicochemical properties of quinoa RS3-type resistant starch (RS3-type QRS) and the

收稿日期: 2025−09−02

基金项目: 黑龙江省“双一流”学科协同创新成果项目（LJGXCG2025-F27）。

作者简介: 王汇（2000−）, 女, 硕士研究生, 研究方向: 食品营养与质量安全, E-mail: 13803901709@163.com。

*** 通信作者:** 姚笛（1980−）, 女, 博士, 教授, 研究方向: 食品生物科学与技术, E-mail: yd13845991700@163.com。

王长远（1976-）, 男, 博士, 教授, 研究方向: 粮食、油脂及植物蛋白工程, E-mail: byndwcy@163.com。

effects of its *in vitro* fermentation on the intestinal flora and short-chain fatty acids (SCFAs), quinoa starch (QS) was prepared via alkali extraction and then autoclaved to obtain RS3-type QRS, and the amylose content, transmittancy, pasting properties, and thermal properties of both starches were analyzed. The *in vitro* fermentation characteristics of the two and their effects on intestinal metabolites were further explored using an *in vitro* fecal simulation fermentation system, 16S rRNA sequencing, liquid chromatography-mass spectrometry, and non-targeted metabolomics. Compared with QS, RS3-type QRS had significantly higher contents of resistant starch and amylose (P<0.05), significantly improved transmittancy and solubility (P<0.05), possessed more stable thermodynamic properties, and was better in quality and easier to cook. After adding RS3-type QRS to the *in vitro* fermentation matrix, the abundance of *Faecalibacterium* increased whereas that of *Escherichia-Shigella* decreased. Members of the Firmicutes, including *Blautia* and *Lactococcus*, formed the core community in RS3-type QRS and were significantly positively correlated with butyric acid enrichment (P<0.01 or P<0.05). In metabolic pathways of bile secretion, the bile acid levels were significantly increased (P<0.05). SCFAs produced by the intestinal flora, together with the differential metabolites, maintained intestinal homeostasis. The findings from this study provide a reference for exploring the impact of RS3-type QRS on intestinal health and a theoretical basis for its application.

Key words: quinoa; RS3 resistant starch; *in vitro* fermentation; intestinal flora; metabolites; bile acids

Quinoa is a plant belonging to the Chenopodiaceae family, which is rich in various vitamins, proteins, phytosterols, and flavonoids and possesses multiple physiological functions. Starch is an important component of quinoa, accounting for 53%~69% of the dry weight of quinoa grains[1]. Starch can be classified into three distinct types: Rapidly digestible starch (RDS), slowly digestible starch (SDS), and resistant starch (RS)[2]. RS refers to starch fractions that cannot be enzymatically degraded in the small intestine but undergo fermentation or partial fermentation in the human gastrointestinal tract and colon, thereby producing short-chain fatty acids (SCFAs)[3]. Based on their source, characteristics, and processing methods, RS can be divided into five categories: RS1 (physically entrapped starch), RS2 (resistant starch granules), RS3 (retrograded starch), RS4 (chemically modified starch), and RS5 (starch-lipid complexes)[2]. Compared with other starch types, RS is more difficult to digest and absorb in the human body, so the calories generated in the body after ingestion are lower. In contrast to other RS types, RS3 has better water-holding capacity and thermal stability[4] and is classified as a type of dietary fiber[5]. Adding RS3 to food does not affect the flavor or color of the product, and its taste is superior to that of traditional dietary fiber. Owing to its excellent physicochemical properties and physiological effects, RS3 is regarded as a promising novel food ingredient[4]. RS3 is the most common type of RS in food; Starchy foods form partial retrograded starch when cooled after cooking, and thermal processing conditions affect the formation and structure of retrograded starch. The autoclave method, the most widely used technique for preparing RS3, employs high pressure and temperature, which can increase the RS content of quinoa starch (QS)[6]. RS exists in many natural foods, such as corn and potatoes. Compared with regular corn starch, QS has a higher amylopectin content, whereas its amylose content is much lower than that of wheat, sorghum, millet, and corn[1]. Intestinal flora can more readily ferment amylopectin and RS in starch, leading to an increase in SCFA content after 24 h of fermentation[7]. As key metabolites of intestinal microorganisms, SCFAs organically link the complex interactions between host diet and intestinal microbiota. SCFAs serve as important energy sources for intestinal epithelial cells and natural ligands for free fatty acid receptors[8], and they exert multiple health-promoting effects, such as regulating lipid metabolism, immunity, and inflammatory responses. These metabolites are mainly produced by utilizing indigestible carbohydrates (including RS, non-starch polysaccharides, and oligosaccharides)[9]. Intestinal flora can produce SCFAs independently or synergistically via different metabolic pathways. Therefore, supplementing RS can not only alter the content of intestinal SCFAs, but also promote intestinal microecological homeostasis and improve intestinal health[10].

Previous studies have mostly focused on the functional exploration and application of quinoa starch and quinoa resistant starch, but research on the relationship between SCFAs produced by the fermentation of QS and quinoa RS3-type resistant starch (RS3-type QRS), and the intestinal microbial community as well as intestinal metabolites remains limited. Thus, this experiment investigated the physicochemical properties and *in vitro* fermentation characteristics of QS before and after high-temperature and high-pressure treatment. It also explored the effects of RS3-type QRS addition on intestinal flora and intestinal microbial metabolism, as well as the intestinal microorgan-

isms and metabolic pathways involved in SCFA production, providing a reference for the application of RS3-type QRS in food products.

1 Materials and methods

1.1 Instruments and equipment

Quinoa was acquired from a local farmer's market Jining, Shandong, China; Acetic acid, propionic acid, and butyric acid (analytical purity) Shanghai McLean Biochemistry Co., Ltd.; Metaphosphoric acid, sulfuric acid (analytically pure) Shanghai Pharmaceutical Group Chemical Reagent Co., Ltd.; Axygen Biosciences DNA Gel Extraction Kit Axygen Biosciences United City, California, USA; E.Z.N.A.® soil DNA kit Omega Bio-tek Knox Norcross, Georgia, USA; Feces were obtained from 6 volunteers (20~25 years old) who had no history of gastrointestinal diseases and antibiotic treatment within three months at Heilongjiang Bayi Agricultural University.

TENSOR II Infrared Spectrometer Tianjin Jinbeier Technology Co., Ltd.; YT-DF200 Paddy quality rapid detector Shandong Yuntang Intelligent Technology Co., Ltd.; Agilent 1200 HPLC Agilent Technologies Inc., USA; A360 UV-visible scanning spectrophotometer AOE Instruments Co., Ltd.; Perkin-Elmer TA DSC25 Platinum Elmer Instruments Inc.; 2194617TMB RVA Perten Instruments Co., Ltd.; miSeq high-throughput sequencing platform Illumina Co., Ltd.; UHPLC Exactive Thermo Fisher Scientific Co., Ltd.

1.2 Experimental methods

1.2.1 Preparation of RS3-type QRS The method for preparing RS3-type QRS was modified based on the QS extraction protocol reported by González-soto et al.[11]. Quinoa grains were first crushed and sieved, then mixed with a 0.2% NaOH solution, and centrifuged to remove impurities. The resulting precipitate was further rinsed with distilled water and centrifuged again to eliminate residual impurities, followed by drying, re-crushing, and sieving to obtain QS. A 26% (w/v) QS suspension was prepared and subjected to high-pressure autoclaving at 121 ℃ for 30 min; Subsequently, the treated mixture was cooled, dried, and ground to yield RS3-type QRS. The RS content was determined in accordance with the method described by Nakayoshi et al.[12].

1.2.2 Physicochemical properties of QS and RS3-type QRS

1.2.2.1 Amylose content The amylose content was determined using a rapid rice quality detector. The experimental procedure was slightly modified according to Yuan et al.[13]. A starch standard solution was first prepared for calibration. The test sample was added to a boiling NaOH solution bath. Thereafter, distilled water, acetic acid solution, and iodine reagent were sequentially added to the sample system, and the absorbance value was measured at a wavelength of 607 nm.

1.2.2.2 Transmittancy The method for determining transmittancy was slightly modified according to Qin et al.[14]. 1% (w/v) suspensions of QS and RS3-type QRS were prepared separately, boiled for a specified duration, and then cooled to room temperature. The absorbance of each sample was quantified at a wavelength of 650 nm using an AOELAB A360 spectrophotometer, and transmittance was calculated based on the absorbance data.

1.2.2.3 Solubility and expansive force Solubility and expansive force were determined in accordance with the method reported by Gao et al.[15]. 10.0% (w/v) starch suspensions of QS and RS3-type QRS were prepared, respectively. Each suspension was incubated in a water bath at 80 ℃ for 30 min, then cooled to room temperature and centrifuged. The obtained supernatant was dried at 105 ℃ to a constant weight. The calculation formulas of solubility and expansive force were as follows:

$$\text{Solubility}(\%)=\frac{m}{m_2}\times 100 \qquad \text{式（1）}$$

$$\text{Expansive force}(g/g)=\frac{m_1}{m_2(1-S)}\times 100 \qquad \text{式（2）}$$

Among them, m denoted the mass of the supernatant after drying (g); m_1 denoted the mass of the precipitate (g); m_2 denoted the mass of the sample (g); S denoted the solubility (%).

1.2.2.4 FTIR spectroscopy of QS and RS3-type QRS The method for FTIR spectroscopy was performed with slight modifications according to Sevenou et al.[16]. QS and RS3-type QRS samples were mixed with KBr, and the wavelength from 4000 to 500 cm^{-1} was scanned using an infrared spectrometer. The alterations in QS and RS3-type QRS chemical bonds were examined.

1.2.2.5 Thermal properties by DSC Thermal properties were determined using a method described by Fang et al.[17] with minor modifications. An aliquot of 2.5 mg of sample was mixed with 5 μL of distilled water in an aluminum pan, with nitrogen used as the inert atmosphere. The temperature range for scanning was set from 25 ℃ to 150 ℃, with a heating rate of

10 ℃/min, and the nitrogen flow rate was maintained at 20 mL/min throughout the test.

1.2.2.6 Gelatinization properties by RVA The pasting properties were determined in accordance with the method described by Liu et al.[18]. An appropriate amount of sample was weighed and prepared into a starch suspension, which was heated to 95 ℃ using RVA, kept warm, and cooled to 50℃ for determination. The peak viscosity (PV), trough viscosity (TV), break down (BD) viscosity, final viscosity (FV), and setback (SB) viscosity were recorded.

1.2.3 Anaerobic fermentation of human feces *in vitro* *In vitro* fecal fermentation was performed using quinoa starch (QS) or RS3-type QRS as the sole carbon source, with the method modified slightly according to Lesmes et al.[19]. Fresh fecal samples were pooled in equal proportions and homogenized in phosphate-buffered saline (PBS) at a ratio of 1∶6 (w/v). The mixture was filtered through sterile gauze to prepare a fecal suspension. For each fermentation system, 0.10 g of QS or RS3-type QRS was separately added, followed by mixing the fecal suspension with YCFA medium at a volume ratio of 1∶9. Three experimental groups were established: QS group, QRS group, and BLANK group (no exogenous carbon source added). Fermentation was carried out under anaerobic conditions. Samples were collected at 0, 6, 12, 18, 24, and 48 h post-fermentation for short-chain fatty acid (SCFA) quantification. After 24 h of fermentation, supernatant aliquots from each group were harvested for genomic DNA extraction.

1.2.4 Determination of SCFAs The concentrations of target SCFAs (acetic acid, propionic acid, and butyric acid) in fermentation samples were quantified following the method reported by Yao et al.[20]. Fermentation broth was mixed with a metaphosphoric acid solution at a volume ratio of 5∶1 and vortexed thoroughly for homogenization. After centrifugation and filtration, the content of SCFAs was determined by the external standard method. Ion exclusion chromatography column (7.8 mm×300 mm, 7 μm), mobile phase: H_2SO_4 solution (2.5% acetonitrile), column temperature and flow rate: 60 ℃, 0.5 mL/min.

1.2.5 16S rRNA gene sequencing Genomic DNA was isolated from the fermentation broth utilizing a DNA extraction kit. The V3~V4 region of the 16S ribosomal RNA gene was amplified employing bacterial primers 338 (FACTCCTACGGGAGGCAGCAG) and 806 R (GGACTACHVGGGTWTCTAAT). PCR amplification was performed in a 50 μL volume using SanTaq PCR Mix, template DNA, primers, and sterile ddH_2O. The thermal cycling conditions were as follows: Initial denaturation at 94 ℃ for 5 min; 35 cycles of 94 ℃ for 30 s, 55 ℃ for 30 s, and 72 ℃ for 30 s, and a final extension at 72 ℃ for 10 min to obtain the PCR products. After PCR products were identified by 2% agarose gel electrophoresis, the gel blocks containing the target bands were dissolved in a dissolution buffer and incubated in a 55 ℃ water bath until they were completely dissolved. The mixture was then subjected to binding to the adsorption column, washing with ethanol, and elution with buffer, thus completing the purification of the PCR products. The Illumina MiSeq platform was used for high-throughput sequencing. The sequence data related to this project was submitted to the NCBI Short Read Archive database (Accession Number: PRJNA1097460). Principal component analysis (PCA), linear discriminant analysis (LDA), and linear discriminant analysis effect size (LEfSe) analysis were performed on the dataset to forecast the functional capabilities of bacterial genomes.

1.2.6 Analysis of metabolites in fermentation broth Metabolites in samples from each group were analyzed via liquid chromatography-mass spectrometry (LC-MS). Metabolite extraction was performed using a methanol-water solution at a volume ratio of 4∶1 (v/v). Sample pretreatment was carried out following the method described by Qi MH (Meiji). Chromatographic separation was conducted on an ACQUITY HSS T3 column (100 mm×2.1 mm, 1.8 μm) at 40 ℃ using a UHPLC Exactive system, with a sample injection volume of 3 μL and a flow rate of 0.40 mL/min; detailed separation conditions followed the protocol reported by Yao et al.[20]. Differential metabolites with statistical significance between groups were screened by VIP value. Metabolic enrichment analysis and pathway analysis (based on database retrieval, KEGG, http://www.genome.jp/kegg/) were performed.

1.3 Statistical analysis

Statistical analysis was conducted using SPSS version 22.0 to determine the significance of differences through ANOVA, with results presented as $\bar{x}\pm s$. The experimental findings were visualized utilizing Origin 64 software.

2 Results and analysis

2.1 Physicochemical properties

2.1.1 Physicochemical properties and FTIR spectra analysis of QS and RS3-type QRS The RS content, amylose content, transmittancy, solubility, and expan-

Table 1 Physicochemical properties analysis of QS and RS3-type QRS

Samples	RS content (%)	amylose content (%)	transmittancy (%)	solubility (%)	expansive force (%)
QS	20.38±0.33^{b}	4.04±0.43^{b}	4.45±0.45^{b}	5.30±0.20^{b}	35.30±0.20^{a}
QRS	23.63±0.43^{a}	7.83±0.47^{a}	18.93±0.15^{a}	35.43±0.15^{a}	12.92±0.96^{b}

Notes: The difference of superscript letters after the same row of values was significant (P<0.05).

sive force of QS and QRS were illustrated in Table 1. Table 1 showed significant differences in RS and amylose contents between QS and QRS (P<0.05). QRS underwent gelatinization and retrogradation via autoclaving, with amylose molecules rearranged. More stable double-helical structures formed via intermolecular hydrogen bonding aggregated into enzyme-resistant crystalline domains[21], which improved resistance to enzymatic hydrolysis and consequently increased RS content[9]. Transmittance directly reflects starch transparency, an important parameter of starchy foods that affects product appearance, consumer acceptance, and processing applicability[22]. Absorbance and transmittance showed a non-linear negative correlation: lower absorbance indicated higher transmittance and better transparency. QS had a transmittance of 4.45%±0.45%, while QRS reached 18.93%±0.15%, with the latter being significantly higher (P<0.05), indicating superior transparency of QRS. Table 1 showed QRS had higher solubility but lower swelling power. This might be because the high-pressure treatment during the preparation process destroyed the crystal structure of starch granules, released some soluble starch, and increased the solubility of QRS[21]. After autoclaving, RS3-type QRS granule structure became more compact, reducing water absorption capacity and leading to lower swelling power[23].

The infrared spectra of QS and QRS were illustrated in Fig.1. After high-temperature and high-pressure treatment, no notable change in absorption peaks was observed for RS3-type QRS, with no significant differences between QS and RS3-type QRS in basic skeleton, chemical groups, or chemical bonds.

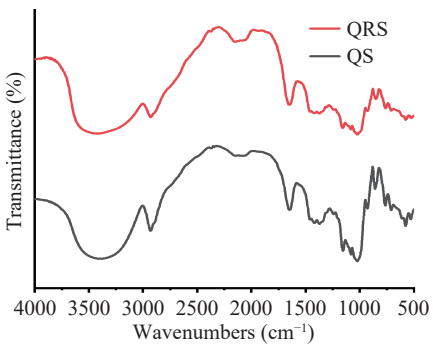


Fig.1 FT-IR spectra of QS and QRS

2.1.2 Thermal Properties of QS and RS3-type QRS

Table 2 presented the findings on the thermodynamic properties of QS and QRS. The gelatinization temperatures (To, Tp, Tc) and gelatinization enthalpy (ΔH) of QS were significantly lower than those of QRS (P<0.05). Previous studies have shown that during RS heating, amylose molecules interact with other molecules to form compact, robust structures. QRS formed a denser crystalline structure, thus requiring higher temperatures and more energy to disrupt its crystalline structure[24].

Table 2 Thermal Properties by DSC

Samples	To (℃)	Tp (℃)	Tc (℃)	ΔH (J/g)
QS	60.59±1.02^{b}	65.88±1.07^{b}	77.49±1.97^{b}	2.55±0.23^{b}
QRS	135.63±1.47^{a}	137.27±2.21^{a}	145.21±2.06^{a}	5.89±0.20^{a}

Notes: The difference of superscript letters after the same row of values was significant (P<0.05).

Compared with other quinoa resistant starch types (RS1-type QRS, RS2-type QRS, RS4-type QRS, and RS5-type QRS), RS3-type QRS had certain advantages in food processing[25]. The QRS prepared via autoclaving is RS3-type QRS[11]. RS3-type QRS had better thermal stability, maintained a stable structure in high-temperature processing such as baking and cooking, and was not easy to over-gelatinize. RS3-type QRS could thicken and form a close network with gluten, improve the hardness and elasticity of noodles, and enhance the texture and taste of noodles[25]. Compared with other types of resistant starch, the effect of RS3-type QRS on increasing satiety was more obvious, which could better meet people's demand for reducing calorie intake.

2.1.3 RVA Analysis of QS and RS3-type QRS The pasting properties of QS and QRS were listed in Table 3. Lower BD suggested improved thermal stability and enhanced shear resistance of the samples[26]. The PV, BD, and SB of QRS were significantly higher than those of QS (P<0.05). The PV reflected the maximum viscosity of starch granules during heating-induced expansion. The amylose recrystallized structure of QRS delayed gelatinization; however, its post-gelatinization swelling was more intense[27]. Thus, QRS had a higher PV and was easier to cook with superior quality. The crystalline structure of QRS was

Table 3　Gelatinization properties by RVA

Samples	PV (cP)	TV (cP)	BD (cP)	FV (cP)	SB (cP)
QS	1975±4.35^{b}	1805±10.78^{a}	170±4.17^{b}	2051±9.17^{a}	246±4.56^{b}
QRS	2021±5.84^{a}	1313±5.56^{b}	708±6.06^{a}	1679±10.02^{b}	366±13.6^{a}

Notes: The difference of superscript letters after the same row of values was significant (P<0.05).

less stable under high-temperature shear conditions; The ordered domains formed by amylose recrystallization were easily disrupted by shear forces, leading to a rapid decline in starch paste viscosity[28]. This explained why RS3-type QRS had a higher BD than QS. The SB reflected the degree of retrogradation of the starch paste during cooling. RS3-type QRS had a higher amylose content, and its amylose molecules were more prone to reorientation and recombination during cooling[29]. As a result, RS3-type QRS exhibited a higher SB than QS.

2.2 Analysis of microbial community composition

The effects of QS and RS3-type QRS on human fecal microbial community composition were evaluated using the Simpson, Chao1, Ace, and Shannon indices (indices reflecting community richness and diversity). There was no significant increase in diversity in the QRS group. No significant differences were observed in the Chao1, Ace, and Shannon indices among the three groups. The results of the Simpson index showed that the community diversity of the QS group was significantly higher than that of the BLANK group (P<0.05), while no significant difference was found between the QRS group and the BLANK group (Table 4).

Table 4　Microbial community α-diversity index

Sample	Chao1	Ace	Shannon	Simpson
BLANK	382.51±50.79^{a}	385.84±55.71^{a}	3.25±0.20^{a}	0.12±0.03^{a}
QS	340.65±23.03^{a}	347.04±27.10^{a}	3.22±0.19^{a}	0.01±0.03^{b}
QRS	353.55±25.29^{a}	360.84±31.33^{a}	3.29±0.14^{a}	0.09±0.02^{a}

Notes: The difference of superscript letters after the same row of values was significant (P<0.05).

Microbial community composition changes were investigated by analyzing the abundance of dominant bacterial populations across the QS, QRS, and BLANK groups. Fig.2A showed that Firmicutes, Bacteroidota, and Proteobacteria were the most abundant bacterial phyla in all samples. Firmicutes plays a key role in butyrate production[30]. The Firmicutes/Bacteroidetes (F/B) ratio was a core indicator reflecting the relative balance of intestinal carbohydrate-degrading flora. The results showed that the F/B ratios of the QS group and QRS group were lower than that of the BLANK group, and QS and QRS were more conducive to the decomposition and utilization of refractory carbohydrates. Additionally, Proteobacteria are typically associated with intestinal flora imbalance[31]; Relative to the BLANK group, both QS and QRS groups had lower Proteobacteria levels, suggesting that intake of QS and QRS helps maintain intestinal flora homeostasis to a certain extent. Fig.2B showed that *Bacteroides*, *Escherichia-Shigella*, and *Faecalibacterium* were the dominant groups in all samples. *Faecalibacterium* could produce abundant butyric acid and propionic acid, maintain intestinal barrier function, and regulate the immune system[32]. *Faecalibacterium* levels were higher in the QS and QRS groups than in the BLANK group. Conversely, the QRS group had significantly lower *Escherichia-Shigella* abundance than the BLANK group (P<0.05). As pathogenic taxa linked to intestinal dysbiosis, the reduced abundance of *Escherichia-Shigella* indicated that RS3-type QRS supplementation could inhibit pathogenic bacterial growth and preserve intestinal homeostasis.

As shown in Fig.2C, the microbial community distribution of the QS and QRS groups was relatively clustered, and both were distinctly separated from the BLANK group, demonstrating that QS and QRS supplementation significantly modulated human intestinal flora structure. The evolutionary branch diagram of LEfSe analysis was used to further explore the effects of QS and QRS on intestinal microbial communities. Fig.2D showed that the diversity of the QRS group was higher than that of the QS group, and each group produced enrichment of different species. The QS group was enriched with bacteria of *Holdemania* and *Moryella*, and the QRS group was enriched with bacteria of Firmicutes, Negativicutes, and Lachnospiraceae. As shown in Fig.2E, the histogram of LDA scores (LDA>3). After fermentation, there were differences in the intestinal dominant flora of the two starch samples. The core species of the QS group was *Bacteroidetes*, while the core species of the RS3-type QRS were Firmicutes and Lachnospirales. Firmicutes were key components of the human intestinal microbiota; they could ferment RS to produce SCFAs, thereby promoting the proliferation of beneficial intestinal bacteria and protecting intestinal health[33]. The higher RS and amylose contents in RS3-type QRS provided fermentation substrates for Firmicutes (e.g., Lachnospirales and *Ruminococcus*), facilitating butyric acid production.

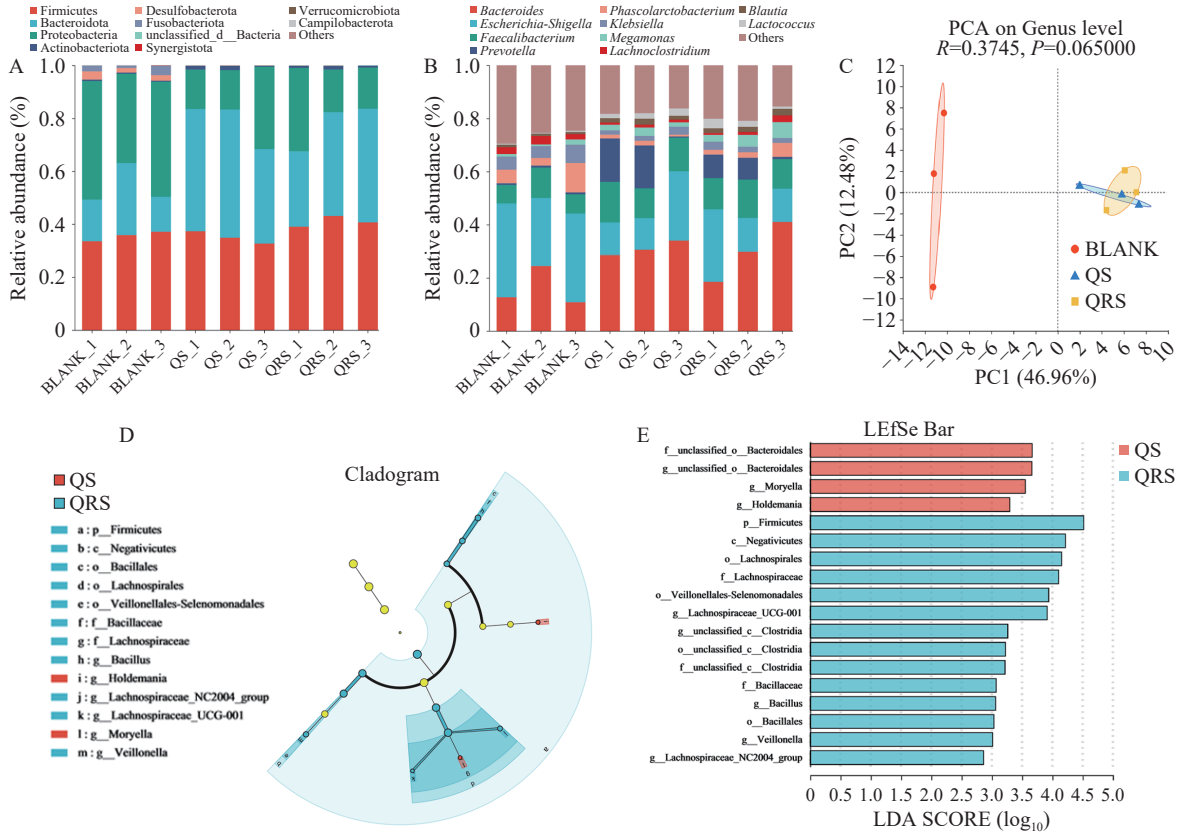


Fig.2 Bacterial community composition of QS and QRS fermentation for 24 h

Notes: A. Phylum level; B. Genus level; C. PCA; D. LEfSe; E. LDA score histogram.

2.3 SCFAs and pH analysis

Intestinal anaerobic bacteria utilized carbohydrates to produce short-chain fatty acids (SCFAs), which could supply energy to colonocytes[11]; SCFAs also regulated intestinal pH, enriched beneficial bacteria, and inhibited pathogenic bacterial growth. Fig.3 showed the changes in SCFAs levels and pH of QS and QRS during different fermentation periods. Fig.3A~Fig.3D indicated that, compared with the QS group, the level of acetic acid in the QRS group was slightly increased, and the levels of butyric acid and total acid were significantly increased (P<0.05), while the level of propionic acid was slightly lower than that in the QS group. The QRS group also had higher relative abundance of Firmicutes than both the QS and BLANK groups, a phenomenon linked to its high RS content. Firmicutes are key butyrate-producing taxa; Prior studies have also shown that fermented RS typically yields higher butyric acid levels. Butyric acid has anti-inflammatory properties, strengthens the colonic barrier, and may reduce colon cancer risk[34]. Fig.3E showed that with the increase of *in vitro* fermentation time, the pH level of the BLANK group gradually declined throughout the entire fermentation process. The pH of the *in vitro* fermentation broth supplemented with QS and RS3-type QRS decreased rapidly from 0 to 6 h. During the same time period, the pH of the BLANK group decreased slowly. This observation might be attributed to the fact that no additional carbon source was added to the BLANK group, whereas QS and QRS, as starch-derived organic carbon sources, were readily fermented by microorganisms, thereby causing a rapid pH decline at this stage. Compared with the QRS group, the pH of the QS group exhibited a significantly greater decrease within this time range (P<0.05). This significant difference could be explained by the lower RS content in QS, which made it more susceptible to microbial decomposition and subsequent acid production. From 6 to 48 h, the pH of both the QS and QRS groups showed a slow recovery trend; However, the final pH of both groups at the end of the entire fermentation process remained lower than their initial pH. This pH recovery might have resulted from shifts in carbon source metabolism and microbial metabolic pathways during late fermentation: Methanogens and syntrophic bacteria in fecal inocula could decompose SCFAs as secondary substrates[35]; Additionally, *Escherichia coli* in fecal broths could ferment carbohydrates to produce SCFAs, and could also cleave carbon dioxide and hydrogen via hydrogenolysis enzyme systems, which might have contributed to the late-stage

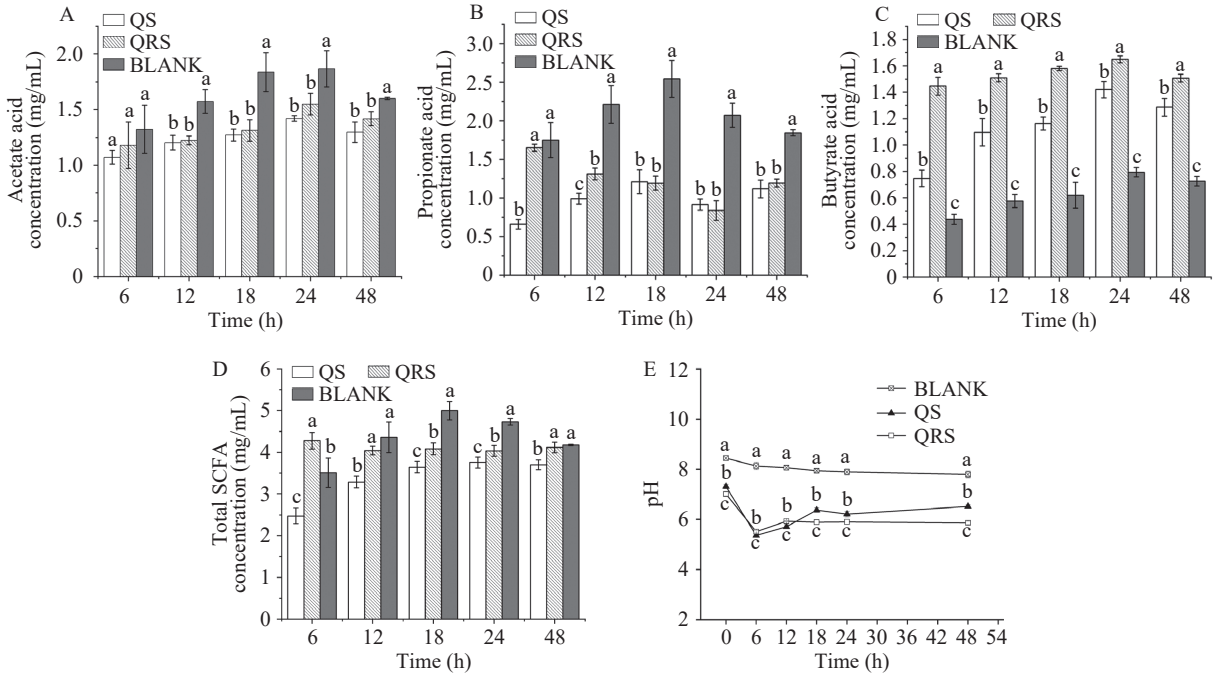


Fig.3　Changes of SCFAs in different periods of *in vitro* fermentation

Notes: A. Acetic acid; B. Propionic acid; C. Butyric acid; D. Total SCFAs; E. pH; The significant difference between different groups was represented by different letters (P<0.05).

pH increase in fermentation broths[36].

Compared with QS, RS3-type QRS resisted gelatinization and disintegration during processing or in the gastric acidic environment due to its favorable thermal stability, which allowed it to reach the large intestine more intact. And its dense structure was decomposed slowly by the flora, which continuously provided substrates for the flora so that SCFAs-producing bacteria (Firmicutes) could colonize and produce SCFAs, especially increased butyric acid production. The high solubility of RS3-type QRS facilitated its dispersion into small-molecular fragments in the large intestine, which increased its contact with intestinal flora and supported the attachment and utilization of amylase secreted by SCFA-producing bacteria. Furthermore, in this acidic environment, dispersed small-molecular fragments were preferentially utilized by beneficial bacteria, which inhibited substrate competition by harmful bacteria and modulated the flora structure[37]. Collectively, the thermal stability and high solubility of RS3-type QRS influenced its intestinal fermentation behavior and jointly regulated metabolite changes.

2.4　Correlation analysis between human intestinal microbial community and SCFAs

Fig.4 was a heatmap depicting the correlation between SCFAs and intestinal bacterial communities. The results showed that *Phascolarctobacterium* and *Lachnoclostridium* were significantly positively correlated with acetic acid production (P<0.01). *Phascolarctobacterium* is an obligate anaerobic Gram-negative bacterium capable of producing acetic acid and propionic acid[38], while *Lachnoclostridium* can generate acetic acid and exerts anti-inflammatory and immunomodulatory effects[39]. *Bacteroides* and *Prevotella* were positively correlated with butyric acid production, and *Megamonas*, *Blautia*, and *Anaerostipes* exhibited a significant positive correlation with butyric acid production (P<0.01). Butyric acid exerts multiple beneficial effects on host health, including anti-inflammatory activity and maintenance of intestinal im-

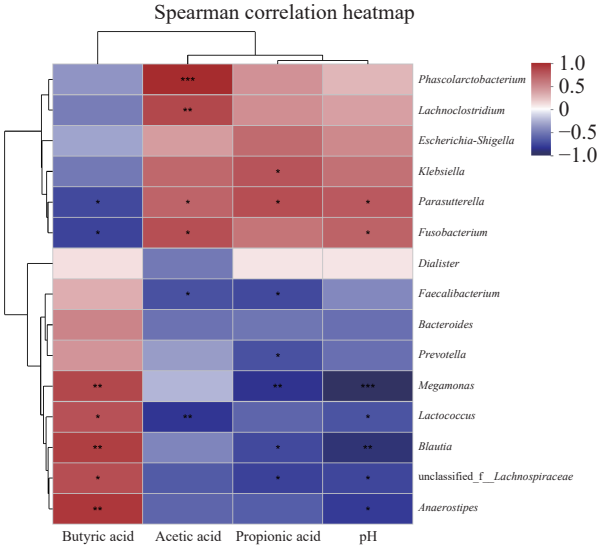


Fig.4　Correlation heat map (intestinal flora and SCFAs)

Notes: ***: P<0.001, **: P<0.01, *: P<0.05.

mune homeostasis[40]. *Megamonas* could metabolize organic nutrients, ferment RS, and produce acetic acid and propionic acid[41]. As a form of RS, RS3-type QRS was extensively utilized by intestinal microbiota in the colon, which facilitated SCFA production by intestinal flora. *Blautia* can enhance colonic mucus function and development via SCFA secretion, thereby helping form a protective microenvironment for intestinal microorganisms. Additionally, human studies have shown that carbohydrate intake is positively associated with butyric acid production and the abundance of butyrate-producing bacteria in *Blautia* populations, indicating that *Blautia* plays a key role in human intestinal butyrate metabolism[42]. A*naerostipes* was a member of the family Lachnospiraceae and one of the main groups producing butyrate in the intestines of humans and animals[43]. The rough surfaces generated by RS starch chain cleavage were rapidly recognized by intestinal flora, which promoted the early-stage enrichment of *Bacteroides* and *Prevotella*. The flora further degraded RS into small molecular fragments, providing substrates for subsequent *Blautia* and *Anaerostipes*, which synergistically promoted the production of butyric acid[44]. *Parasutterella* showed a strong positive correlation with propionic acid production (P<0.05), and its abundance is linked to RS supplementation[45]. This indicated that the addition of QRS could promote the fermentation of intestinal microorganisms to produce more SCFAs, and the intestinal microorganisms could synergistically promote the production of SCFAs and contribute to intestinal homeostasis. The buildup of SCFAs resulted in a lower pH, suppressed the growth of harmful microbes, and helped preserve the balance of intestinal microorganisms.

2.5 Enrichment analysis of differential metabolites between different groups

Fig.5A~Fig.5C were volcano plots of differential metabolites between groups (P<0.05). Compared with the BLANK group, the QS group had more down-regulated differential metabolites (141) (Fig.5A), while the QRS group had more up-regulated differential metabolites (269) (Fig.5B). Relative to the QRS group, the QS group exhibited 75 down-regulated and 42 up-regulated metabolites (Fig.5C). Notably, the QRS group showed a significant increase in differential metabolite count compared with the BLANK group. Moreover, RS3-type QRS supplementation enhanced intestinal microbial community diversity and increased the variety of differential metabolites, highlighting the key role of RS intake in elevating intestinal microbial diversity and improving human intestinal health. Fig.5D~Fig.5F showed the relative abundance of metabolites between different groups. Lignans, neolignans and their derivatives, hydrocarbon derivatives, and organic sulfur compounds were detected in both the QS vs. BLANK and QRS vs. BLANK comparisons (Fig.5D, Fig.5E), whereas organic sulfur compounds were exclusive to the QS and QRS groups (Fig. 5F). Quinoa seeds naturally contain sulfur-containing compounds (glutathione), and RS can significantly increase sulfate-reducing bacterialpopulations and facilitate hydrogen sulfide synthesis by modulating intestinal microbial composition[46]. Organic acids and their derivatives were highly abundant in all comparison groups.

Fig.5G was a heatmap of differential metabolites in QS and QRS groups, screened by VIP>2 and P<0.05. The QS group had high levels of alkaloids and their derivatives, with organic oxygen compounds (including tropine, nitroflurbiprofen, and myo-inositol) being the dominant class. Tropine is a common intermediate for synthesizing various bioactive alkaloids; Studies have found that natural bioactive alkaloids and polyphenols exhibit strong *in vitro* amylase inhibitory activity but are readily degraded *in vivo*[47], suggesting that the amylase inhibitory activity of RS3-type QRS might have decreased after autoclaving. Myo-inositol could be endogenously formed by glucose decomposition and exists in foods[48]. Compared with the QS group, the QRS group had higher concentrations of benzene ring-containing substances and organic nitrogen compounds. The notable differential metabolite was (3a,5b,7a,12a)-24-[(carboxymethyl)amino]-1,12-dihydroxy-24-oxocholan-3-yl-b-D-Glucopyranosiduronic acid (VIP>2, P<0.05), which was a conjugated bile acid (a glucuronidation product) and belonged to the secondary metabolites of bile acid metabolism[49]. RS fermentation produced SCFAs to reduce intestinal pH, inhibited the passive absorption of bile acids, promoted the formation of conjugated bile acids, and enriched Bacteroidetes and Firmicutes[50]. Furthermore, studies showed that RS intervention could increase fecal conjugated bile acid excretion[51]. As shown in Fig.3, the QRS group had significantly higher butyric acid production than other groups (P<0.05). RS intervention could promote the proliferation of SCFA-producing bacteria, regulate colonic epithelial energy metabolism via SCFAs, and protect the intestinal barrier.

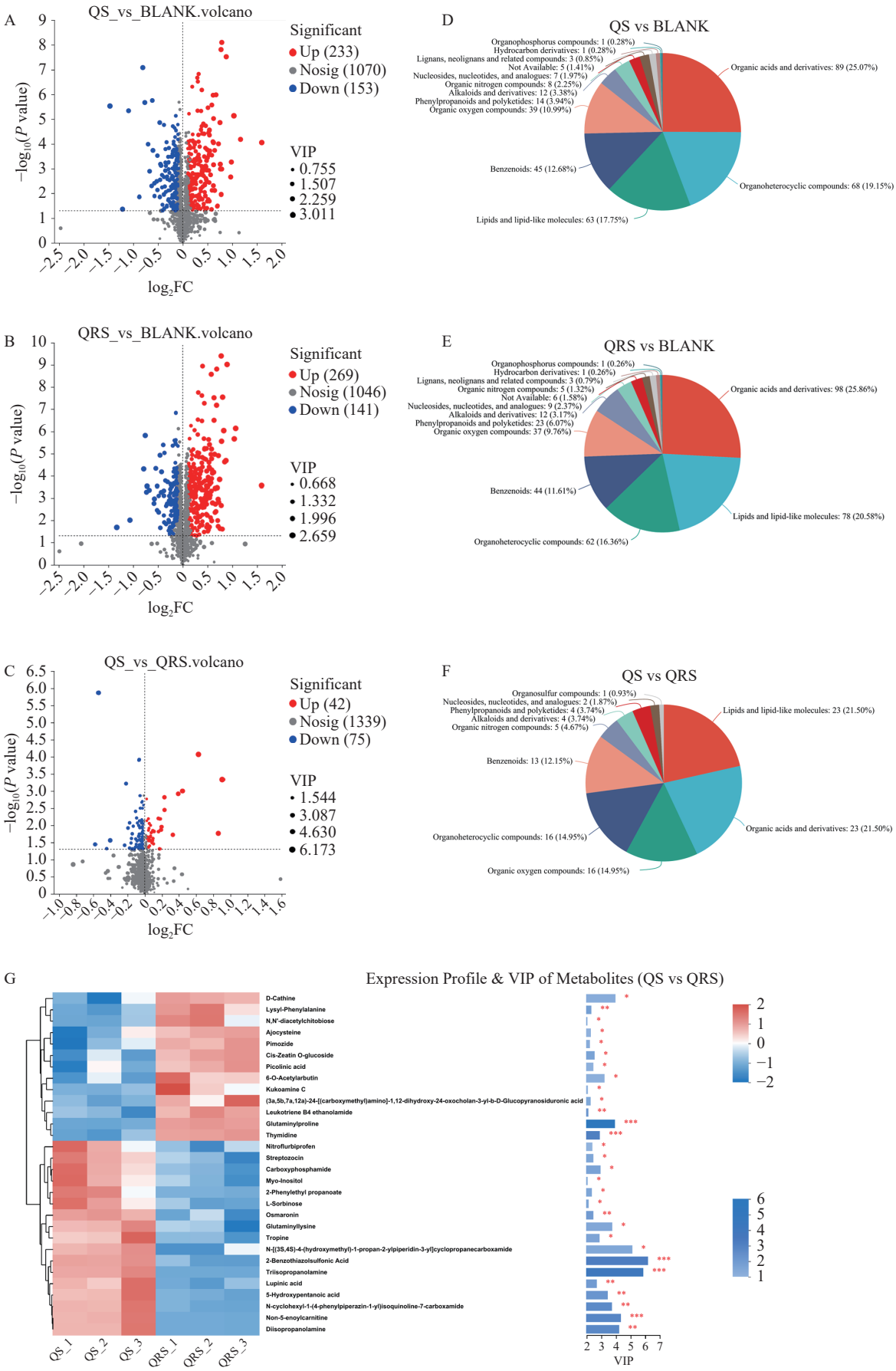


Fig.5　Metabolite compounds by liquid chromatography-mass spectrometry

Notes: Differential metabolite volcano plot (A: QS vs. BLANK, B: QRS vs. BLANK, C: QS vs. QRS). Relative abundance of differential metabolites (D: QS vs. BLANK, E: QRS vs. BLANK, F: QS vs. QRS). Importance of differential metabolites and expression trend change VIP value (G: QS vs. QRS).

2.6 KEGG compound annotation and metabolic pathway enrichment analysis of differential metabolites

Fig.6A~Fig.6C illustrated the analysis of the KEGG secondary metabolic pathway functions pertaining to the differential metabolites observed among the various groups. The results showed that metabolites annotated to metabolic pathways accounted for the largest proportion across all groups, with 128, 135, and 49 differential metabolites identified in each group, respectively. Fig.6D~Fig.6F presented the results of metabolic pathway enrichment analysis for the differential metabolites between groups. The findings indicated that relative to the BLANK group, both the QS and QRS groups were significantly enriched in the bile secretion and *β*-alanine metabolism pathways (P<0.01) (Fig.6D~Fig.6E). Bile acids are important metabolites that regulate intestinal absorption and bile secretion. They can alleviate chronic liver disease and obesity, directly disrupt bacterial cell membranes, create a niche favorable for Firmicutes, and inhibit the proliferation of bile acid-tolerant microorganisms (e.g., Bacteroidetes and Actinobacteria)[52]. Studies have shown that RS intake can ameliorate obesity by modulating intestinal flora-mediated regulation of bile acid composition[53]. Compared with QS, RS3-type QRS had a higher RS content; After ingestion, intestinal flora in the QRS group exhibited enriched Firmicutes, which established a favorable metabolic microenvironment for bile secretion and maintained metabolic homeostasis. As shown in Fig.4, the abun-

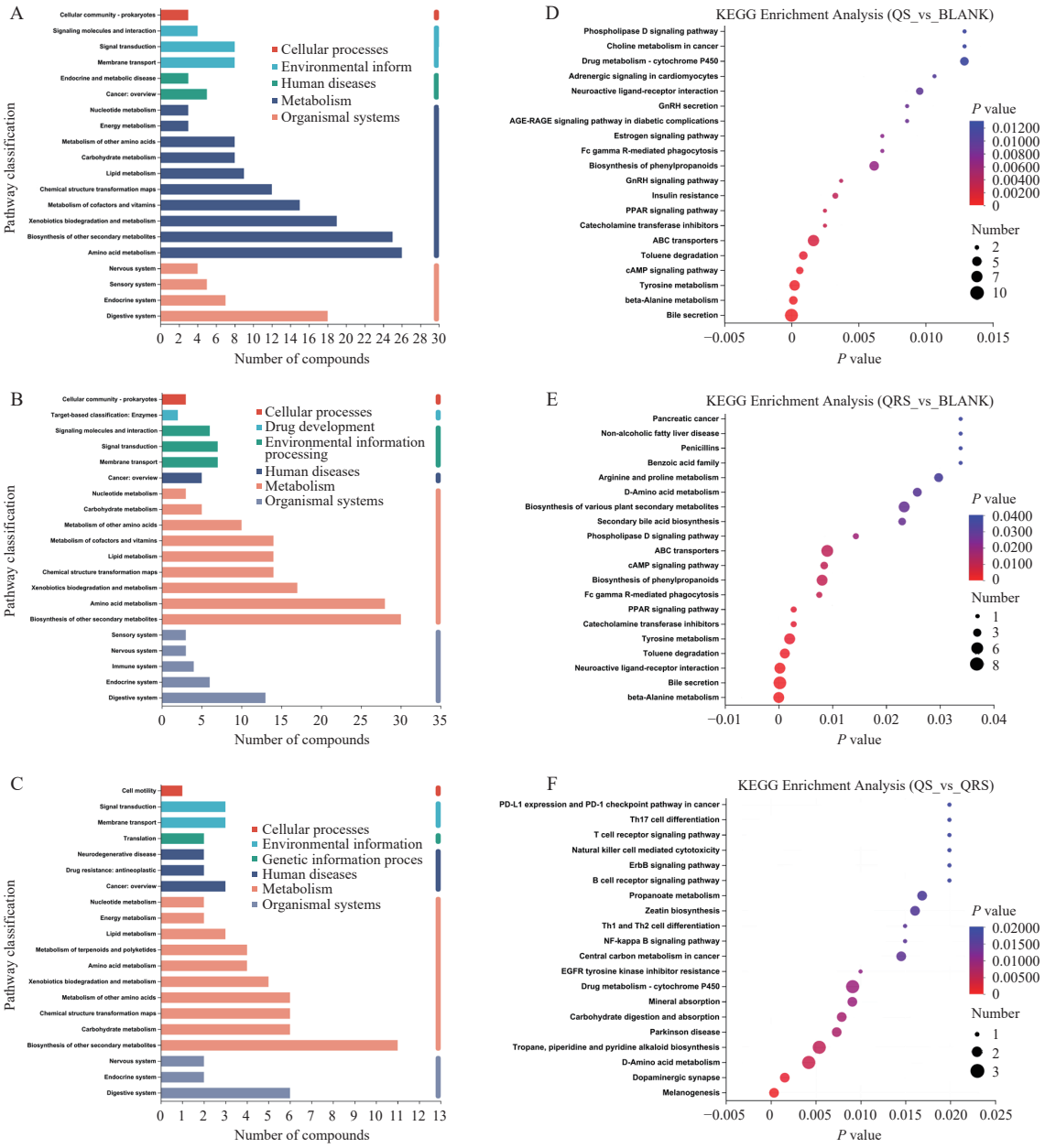


Fig.6 KEGG functional annotation and metabolic pathway enrichment analysis of differential metabolites

Notes: A: QS vs. BLANK, B: QRS vs. BLANK, C: QS vs. QRS, D: QS vs. BLANK, E: QRS vs. BLANK, F: QS vs. QRS.

dance of *Parasutterella* was significantly positively correlated with butyric acid production (P<0.05). Relative to the BLANK group, more metabolites in the QRS group were enriched in the bile secretion pathway. Studies have demonstrated that *Parasutterella* is a succinic acid-producing strain, with a positive correlation between the bacterium's abundance and succinic acid levels; succinic acid is an intermediate in microbial propionic acid synthesis[54]. In addition, the tyrosine metabolism pathway was also significantly enriched in the RS3-type QRS group (P<0.01). Tyrosine is metabolized by intestinal bacteria, and its metabolite p-cresol has garnered attention due to its impacts on host-microbiota interactions[55]. Both QS and QRS groups were significantly enriched in the melanin production and D-amino acid metabolism pathways (P<0.01) (Fig.6F). Studies have shown that some melanin-producing bacteria and some melanin can be anti-inflammatory and regulate the immune regulation[56]. D-amino acids are key components of bacterial cell wall peptidoglycan, which are involved in biofilm degradation; additionally, some D-amino acids exert antibacterial effects[57]. Certain D-amino acid metabolites (e.g., glutamine, glutamic acid) can be further fermented by intestinal bacteria into acetic acid and propionic acid[57], and their combined actions maintain intestinal microbial homeostasis.

2.7 Correlation between key intestinal microbiome and differential metabolites

To explore the association between key intestinal microorganisms and differential metabolites, a Spearman correlation heatmap of intestinal microflora and intestinal metabolites was generated (Fig.7). The results indicated that *Fusicatenibacter* was significantly positively correlated with deoxycholic acid and DL-norvaline (P<0.001). *Fusicatenibacter* played a significant role in the fermentation metabolism of carbohydrates. This genus was capable of utilizing substrates such as glucose and RS to generate SCFAs, including acetic acid, via the glycolytic pathway. DL-norvaline was involved in glucose metabolism. Clinical evidence showed that *Fusicatenibacter* abundance was reduced in the intestines of patients with ulcerative colitis but elevated in healthy individuals[58]. Deoxycholic acid and butyric acid were metabolites of intestinal microbiota that can induce the synthesis of host defense peptides and alleviate intestinal mucosal damage; high deoxycholic acid concentrations are closely linked to bile acid metabolic pathways[59]. Notably, a high-fat diet increases hepatic bile flow, promotes lipid absorption, and impairs intestinal barrier function. Research indicated that *Fusicatenibacter* was a significant producer of butyric acid within the intestinal microbiota, with its abundance exhibiting a positive correlation to the levels of butyric acid found in fecal matter. In addition, the addition of RS4 significantly increased the concentration of deoxycholic acid, and the concentration of deoxycholic acid was positively correlated with the abundance of *Fusicatenibacter*[60], indicating that bile acid metabolism might regulate the activity of the genus. Further, metabolites derived from RS3-type QRS fermentation were intricately linked to bile secretion metabolic pathways. As observed in the present study, the RS3-type QRS group had the highest butyric acid production among the three groups (P<0.05) (Fig.3C). Thus, RS3-type QRS ingestion may indirectly enhance butyric acid synthesis by promoting the proliferation of butyrate-producing bacteria such as *Fusicatenibacter*; the butyric acid generated via RS3-type QRS fermentation could further mitigate intestinal inflammation, thereby forming a positive feedback loop that sustains intestinal homeostasis. *Blautia* and *Anaerostipes* were positively correlated with cucurbitacin B and leucinic acid but negatively correlated with deoxycholic acid (P<0.05). Both *Blautia* and *Anaerostipes* could ferment carbohydrates to produce SCFAs, particularly acetic acid. Cucurbitacin B is a naturally occurring triterpenoid with diverse bioactivities, including alleviation of inflammatory joint disorders, improvement of central nervous system diseases, anti-tumor effects, anti-diabetic activity, anti-inflammation, and anti-oxidation[61]. Leucine can promote mucosal healing in ulcerative colitis; this amino acid may modulate multiple metabolic pathways by regulating intesti-

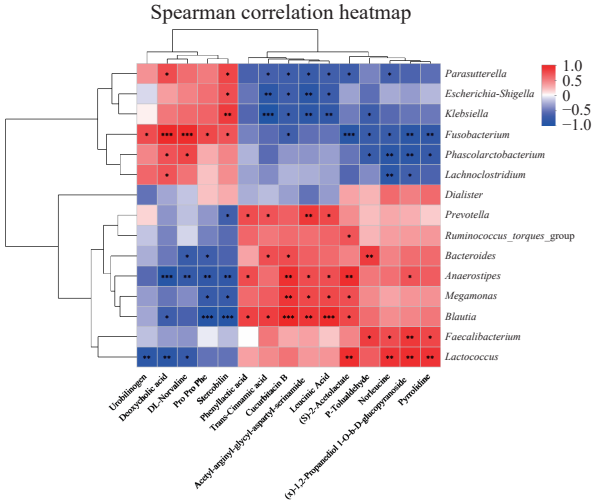


Fig.7　Correlation heat map (intestinal flora and metabolites)
Notes: ***: P<0.001, **: P<0.01, *: P<0.05.

nal microorganisms (e.g., *Blautia*, *Lactobacillus*, and *Bifidobacterium*), participate in intestinal epithelial metabolism, and accelerate ulcerative colitis mucosal repair[62]. Triterpenoids (quinoa saponins) in quinoa can regulate intestinal microbial diversity and promote the proliferation of Firmicutes[63]. *Klebsiella* exhibited a significant negative correlation with trans-cinnamic acid (P<0.05). *Klebsiella* is a Gram-negative bacterium, while trans-cinnamic acid is a phenylalanine metabolite with broad-spectrum antibacterial activity against pathogenic microbes, along with its derivatives[64]. Collectively, RS3-type QRS fermentation inhibited pathogenic bacteria (*Klebsiella*) and enhanced intestinal barrier function, as well as metabolic homeostasis, by increasing the abundance of beneficial butyrate-producing bacteria (i.e., *Fusicatenibacter*, *Blautia*, and *Anaerostipes*). Metabolites including deoxycholic acid, DL-norvaline, and trans-cinnamic acid were closely associated with bile acid metabolism and amino acid fermentation; their synergistic actions collectively improved intestinal barrier integrity, metabolic health, and inflammatory status.

3 Conclusion

In summary, compared with QS, RS3-type QRS had more stable thermodynamic properties, better light transmittance, and superior solubility. The addition of QRS to the *in vitro* fermentation matrix could regulate the structure of human intestinal flora, prevent the proliferation of harmful bacteria (*Escherichia-Shigella*), promote the growth of Firmicutes, create a good metabolic environment for bile secretion, and enhance the production of SCFAs (butyric acid) to maintain the homeostasis of intestinal flora and metabolic homeostasis. Furthermore, bile acids generated via intestinal microbial fermentation of RS3-type QRS showed enhanced involvement in key metabolic processes such as bile secretion. Overall, RS3-type QRS positively influenced the intestinal microbiome and its metabolites, showing the potential of prebiotics, which provided a theoretical basis and experimental support for its food development and utilization.

© The Author(s) 2026. This is an Open Access article distributed under the terms of the Creative Commons Attribution License (https://creativecommons.org/licenses/by-nc-nd/4.0/).

参考文献

[1] LIU H, TIAN G, GAO S, et al. Understanding the changes in multi-structure, physicochemical properties, and *in vitro* digestibility of quinoa starch by annealing with hydrogen-infused and plasma-activated water samples[J]. Journal of Future Foods, 2026, 6(2): 292−300.

[2] WANG M, LIU G, LI J, et al. Structural and physicochemical properties of resistant starch under combined treatments of ultrasound, microwave, and enzyme[J]. International Journal of Biological Macromolecules, 2023, 232: 123331.

[3] MIRJANA R-S, HAUKE S, M D V W. Diversity of the human gastrointestinal tract microbiota revisited[J]. Environmental Microbiology, 2007, 9(9): 2125−2136.

[4] ZHANG Z, BAO J. Recent advances in modification approaches, health benefits, and food applications of resistant starch [J]. Starch-Stärke, 2021, 75(9−10).

[5] WALSH S K, LUCEY A, WALTER J, et al. Resistant starch-an accessible fiber ingredient acceptable to the western palate[J]. Comprehensive Reviews in Food Science and Food Safety, 2022, 21(3): 2930−2955.

[6] REDDY C K, HARIPRIYA S, MOHAMED A N, et al. Preparation and characterization of resistant starch III from elephant foot yam (*Amorphophallus paeonifolius*) starch[J]. Food Chemistry, 2014, 155: 38−44.

[7] ZHOU D, MA Z, HU X. Isolated pea resistant starch substrates with different structural features modulate the production of short-chain fatty acids and metabolism of microbiota in anaerobic fermentation *in vitro*[J]. Journal of Agricultural and Food Chemistry, 2021, 69(18): 5392−5404.

[8] TAN J, MCKENZIE C, POTAMITIS M, et al. The role of short-chain fatty acids in health and disease[J]. Advances in Immunology, 2014, 121: 91−119.

[9] TOPPING D L, CLIFTON P M. Short-chain fatty acids and human colonic function: roles of resistant starch and nonstarch polysaccharides[J]. Physiological Reviews, 2001, 81(3): 1031−1064.

[10] DUNCAN S H, CONTI E, RICCI L, et al. Links between diet, intestinal anaerobes, microbial metabolites and health[J]. Biomedicines, 2023, 11(5): 1338.

[11] GONZÁLEZ-SOTO R A, MORA-ESCOBEDO R, HERNÁNDEZ-SÁNCHEZ H, et al. The influence of time and storage temperature on resistant starch formation from autoclaved debranched banana starch[J]. Food Research International, 2007, 40(2): 304−310.

[12] NAKAYOSHI Y, NAKAMURA S, KAMEO Y, et al. Measurement of resistant starch content in cooked rice and analysis of gelatinization and retrogradation characteristics[J]. Bioscience, Biotechnology and Biochemistry, 2015, 79(11): 1860−1866.

[13] YUAN S M, MIN G C, YUAN J, et al. Research and application of rapid detection method for amylose in rice[J]. Journal of the Chinese Cereals and Oils Association, 2020, 35(10): 169−175.

[14] QIN J, LU R. Measurement of the absorption and scattering properties of turbid liquid foods using hyperspectral imaging[J]. Applied Spectroscopy, 2007, 61(4): 388−396.

[15] GAO L, WANG H, WAN C, et al. Structural, pasting and thermal properties of common buckwheat (*Fagopyrum esculentum* Moench) starches affected by molecular structure[J]. International Journal of Biological Macromolecules, 2020, 156: 120−126.

[16] SEVENOU O, HILL S E, FARHAT I A, et al. Organisation of the external region of the starch granule as determined by infrared spectroscopy[J]. International Journal of Biological Macromolecules, 2002, 31(1-3): 79−85.

[17] FANG G H, DENG X B, TAO Y, et al. Study on the charac-

teristics of resistant starch from two jackfruit seeds[J]. Light Industry Science and Technology, 2019, 35(7): 1−3,37.
[18] LIU X, ZHAO X, MA C, et al. Effects of extrusion technology on physicochemical properties and microstructure of rice starch added with soy protein isolate and whey protein isolate[J]. Foods, 2024, 13(5): 764.
[19] LESMES U, BEARDS E J, GIBSON G R, et al. Effects of resistant starch type III polymorphs on human colon microbiota and short chain fatty acids in human gut models[J]. Journal of Agricultural and Food Chemistry, 2008, 56(13): 5415−5421.
[20] YAO D, WU M, DONG Y, et al. *In vitro* fermentation of fructooligosaccharide and galactooligosaccharide and their effects on gut microbiota and SCFAs in infants[J]. Journal of Functional Foods, 2022, 99: 105329.
[21] SINGH N, SINGH J, KAUR L, et al. Morphological, thermal and rheological properties of starches from different botanical sources[J]. Food Chemistry, 2003, 81(2): 219−231.
[22] APRIANITA A, VASILJEVIC T, BANNIKOVA A, et al. Physicochemical properties of flours and starches derived from traditional Indonesian tubers and roots[J]. Journal of Food Science and Technology, 2014, 51(12): 3669−3679.
[23] PENG M, YIN L, DONG J, et al. Physicochemical characteristics and *in vitro* digestibility of starches from colored quinoa (*Chenopodium quinoa*) varieties[J]. Journal of Food Science, 2022, 87(5): 2147−2158.
[24] YUAN Y, CHAI Z, ZHENG Y, et al. Effect of hawthorn polyphenol extracts on the physicochemical properties and digestibility of corn starch[J]. Journal of Food Science, 2024, 89(3): 1337−1346.
[25] NIU H, ZHAO F, JI W, et al. Structural, physicochemical properties and noodle-making potential of quinoa starch and type 3, type 4, and type 5 quinoa resistant starch[J]. International Journal of Biological Macromolecules, 2024, 258(PT 1): 128772.
[26] ONWULATA C I, TUNICK M H, THOMAS - GAHRING A E. Pasting and extrusion properties of mixed carbohydrate and whey protein isolate matrices[J]. Journal of Food Processing and Preservation, 2014, 38(4): 1577−1591.
[27] YANG L, LIU Y, WANG S, et al. The relationship between amylopectin fine structure and the physicochemical properties of starch during potato growth[J]. International Journal of Biological Macromolecules, 2021, 182: 1047−1055.
[28] JIA B, DEVKOTA L, SISSONS M, et al. Degradation of starch in pasta induced by extrusion below gelatinization temperature[J]. Food Chemistry, 2023, 426: 136524.
[29] ZHU F. Relationships between amylopectin internal molecular structure and physicochemical properties of starch[J]. Trends in Food Science and Technology, 2018, 78: 234−242.
[30] MURUGESAN R, KUMAR J, LEELA K V, et al. The role of gut microbiota and bacterial translocation in the pathogenesis and management of type 2 diabetes mellitus: Mechanisms, impacts, and dietary therapeutic strategies[J]. Physiology and Behavior, 2025, 293: 114838.
[31] RIZZATTI G, LOPETUSO L R, GIBIINO G, et al. Proteobacteria: a common factor in human diseases[J]. BioMed Research International, 2017, 2017: 9351507.
[32] MIQUEL S, MARTÍN R, ROSSI O, et al. *Faecalibacterium prausnitzii* and human intestinal health[J]. Curr Opin Microbiol, 2013, 16(3): 255−261.
[33] YOO S, JUNG S C, KWAK K, et al. The role of prebiotics in modulating gut microbiota: Implications for human health[J]. International Journal of Molecular Sciences, 2024, 25(9): 4834.
[34] WONG J M W, DE SOUZA R, KENDALL C W C, et al. Colonic health: Fermentation and short chain fatty acids[J]. Journal of Clinical Gastroenterology, 2006, 40(3): 235-243.
[35] CLARENS M, MOLETTA R. Kinetic studies of acetate fermentation by *Methanosarcina* sp. MSTA-1[J]. Applied Microbiology and Biotechnology, 1990, 33(2): 239−244.
[36] ROZALEM ARANHA M, IULITA M F, MONTAL V, et al. Basal forebrain atrophy along the alzheimer's disease continuum in adults with down syndrome[J]. Alzheimers Dement, 2023, 19(11): 4817−4827.
[37] CHEN R, ZHANG C, XU F, et al. Meta-analysis reveals gut microbiome and functional pathway alterations in response to resistant starch[J]. Food and Function, 2023, 14(11): 5251−5263.
[38] FEIFAN W, XIANFENG G, JIACHUN Z, et al. *Phascolarctobacterium faecium* abundant colonization in human gastrointestinal tract[J]. Experimental and Therapeutic Medicine, 2017, 14(4): 3122−3126.
[39] LIN K, PENGTAO L, DANYANG W, et al. Alterations in intestinal microbiota diversity, composition, and function in patients with sarcopenia[J]. Scientific Reports, 2021, 11(1): 4628−4628.
[40] TOSHIHIKO T, TAKASHI K, HIROKAZU T, et al. *Fusicatenibacter saccharivorans* gen. nov. , sp. nov. , isolated from human faeces[J]. International Journal of Systematic and Evolutionary Microbiology, 2013, 63(Pt 10): 3691-3696.
[41] YACHIDA S, MIZUTANI S, SHIROMA H, et al. Metagenomic and metabolomic analyses reveal distinct stage-specific phenotypes of the gut microbiota in colorectal cancer[J]. Nature Medicine, 2019, 25(6): 968−976.
[42] HOLMBERG S M, FEENEY R H, PRASOODANAN P K V, et al. The gut commensal *Blautia* maintains colonic mucus function under low-fiber consumption through secretion of short-chain fatty acids[J]. Food Research and Development, 2024, 15(1): 3502−3502.
[43] KADOWAKI R, TANNO H, MAENO S, et al. Spore-forming properties and enhanced oxygen tolerance of butyrate-producing *Anaerostipes* spp[J]. Anaerobe, 2023, 82: 102752.
[44] CHANG D, HU X, MA Z. Comparative study of *in vitro* colonic fermentation dynamics: Human gut microbiota response to resistant starch derived from germinated and extruded pea seeds[J]. Food Hydrocolloids, 2026, 172: 112038.
[45] METZLER-ZEBELI B U, SCHMITZ-ESSER S, MANN E, et al. Adaptation of the cecal bacterial microbiome of growing pigs in response to resistant starch type 4[J]. Applied and Environmental Microbiology, 2015, 81(24): 8489−8499.
[46] YANG X, DARKO K O, HUANG Y, et al. Resistant starch regulates gut microbiota: structure, biochemistry and cell signalling [J]. Cell Physiol Biochem, 2017, 42(1): 306−318.
[47] LIANG Y, CHEN S. Two alkaloids as α-amylase inhibitors: Enzyme kinetics and molecular modeling investigations[J]. Journal of Chinese Pharmaceutical Sciences, 2015, 24(2): 80-87.
[48] MACFARLANE, PETER M, DI F, et al. Myo-inositol effects on the developing respiratory neural control system[J]. Advances in Experimental Medicine and Biology, 2018, 1071: 159−166.
[49] PERREAULT M, BIAŁEK A, TROTTIER J, et al. Role of glucuronidation for hepatic detoxification and urinary elimination of toxic bile acids during biliary obstruction[J]. Public Library of Science ONE, 2013, 8(11): e80994.

[50] DONOHOE D R, GARGE N, ZHANG X, et al. The microbiome and butyrate regulate energy metabolism and autophagy in the mammalian colon[J]. Cell Metabolism, 2011, 13(5): 517−526.
[51] DONGOWSKI G, JACOBASCH G, SCHMIEDL D. Structural stability and prebiotic properties of resistant starch type 3 increase bile acid turnover and lower secondary bile acid formation [J]. Journal of Agricultural and Food Chemistry, 2005, 53(23): 9257−9267.
[52] CANI, PATRICE, DELZENNE, et al. Bile acid metabolism and signaling, the microbiota, and metabolic disease[J]. Pharmacology and Therapeutics, 2022, 237: 108238−108238.
[53] ZENG H, HE S, XIONG Z, et al. Gut microbiota-metabolic axis insight into the hyperlipidemic effect of lotus seed resistant starch in hyperlipidemic mice[J]. Carbohydrate Polymers, 2023, 314: 120939−120939.
[54] CANFORA E E, MEEX R C, VENEMA K, et al. Gut microbial metabolites in obesity, NAFLD and T2DM[J]. Nature Reviews Endocrinology, 2019, 15(5): 261−273.
[55] LETERTRE M P M, MYRIDAKIS A, WHILEY L, et al. A targeted ultra performance liquid chromatography-tandem mass spectrometric assay for tyrosine and metabolites in urine and plasma: application to the effects of antibiotics on mice[J]. Journal of Chromatography B: Analytical Technologies in the Biomedical and Life Sciences, 2020, 1164: 122511.
[56] ZHANG Y G, MALO M E, TSCHIRHART T, et al. Effects of melanized bacteria and soluble melanin on the intestinal homeostasis and microbiome *in vivo*[J]. Toxics, 2022, 11(1): 13.
[57] VAN D A P, GHYSELINCK J, MARZORATI M, et al. The effect of amino acids on production of scfa and bcfa by members of the porcine colonic microbiota[J]. Microorganisms, 2022, 10(4): 762.
[58] TAKESHITA K, MIZUNO S, MIKAMI Y, et al. A single species of *Clostridium* subcluster XIVa decreased in ulcerative colitis patients[J]. Inflammatory Bowel Diseases, 2016, 22(12): 2802−2810.
[59] KIM D M, LIU J, WHITMORE M A, et al. Two intestinal microbiota-derived metabolites, deoxycholic acid and butyrate, synergize to enhance host defense peptide synthesis and alleviate necrotic enteritis[J]. Journal of Animal Science and Biotechnology, 2024, 15(1): 29.
[60] DHAKAL S, DEY M. Resistant starch type-4 intake alters circulating bile acids in human subjects[J]. Frontiers in Nutrition, 2022, 9: 930414.
[61] KUMAR V. Pulmonary innate immune response determines the outcome of inflammation during pneumonia and sepsis-associated acute lung injury[J]. Frontiers in Immunology, 2020, 11: 1722.
[62] YASUTOMI E, INOKUCHI T, HIRAOKA S, et al. Leucine-rich alpha-2 glycoprotein as a marker of mucosal healing in inflammatory bowel disease[J]. Scientific Reports, 2021, 11(1): 11086.
[63] HUANG H, JIA C, CHEN X, et al. Progress in research on the effects of quinoa (*Chenopodium quinoa*) bioactive compounds and products on intestinal flora[J]. Frontiers in Nutrition, 2024, 11: 1308384.
[64] ASLIHAN O T K, HATICE Ö K, ELS Y, et al. Functional groups matter: metabolomics analysis of *Escherichia coli* exposed to trans-cinnamic acid and its derivatives unveils common and unique targets[J]. World Journal of Microbiology and Biotechnology, 2023, 40(2): 47−47.